Comprehensive Assessment of Plasma-Derived circ_0004771 as a Potential Biomarker in Tracking the Progression of Gastric Cancer

Yanhua Xu
Affiliated Hospital of Nantong University
Shan Kong
Affiliated Hospital of Nantong University
Xinyue Qin
Affiliated Hospital of Nantong University
Shaoqing Ju (1564917365@qq.com)
Affiliated Hospital of Nantong University https://orcid.org/0000-0002-2483-7695

Primary research

Keywords: Circular RNA, Circ_0004771, Biomarker, Gastric cancer, Diagnosis

Posted Date: June 22nd, 2020

DOI: https://doi.org/10.21203/rs.3.rs-36545/v1

Abstract

Background: Due to the lack of specific and sensitive detection indicators, most patients with gastric cancer (GC) are already in the advanced stage at the time of diagnosis, resulting in a higher mortality. Therefore, it is urgent to search for effective diagnostic biomarkers with high specificity that can be applied in clinic.

Methods: We screened out circ_0004771 through circRNA sequencing performed on three pairs of GC tissues and corresponding paracancerous tissues. Both exonuclease digestion assay, agarose gel electrophoresis (AGE) and sanger sequencing verified the potential of circ_0004771 being a biomarker. Additionally, we established quantitative real-time fluorescent Polymerase Chain Reaction (qRT-PCR) to detect the expression level of circ_0004771 and evaluated the methodology. What's more, we collected plasma samples from GC patients, precancerous patients and gastritis patients, and we constructed the receiver operating characteristic curve (ROC) to appraise its diagnostic efficacy. Meanwhile, we collected the clinicopathological data of the patients to analyze the relationship between the expression level of circ_0004771 and the pathological parameters of the patients.

Results: The expression level of circ_0004771 is up-regulated both in GC tissues and cells compared to normal controls. Circ_0004771 can be served as a promising biomarker because of its stable cyclic structure and longer half-life. The expression level of plasma circ_0004771 can distinguish between GC patients and precancerous patients, GC patients and gastritis patients. The diagnostic efficiency of circ_0004771 is higher than that of CEA and CA199. Higher diagnostic efficiency can be achieved in combination diagnosis. The expression level of plasma circ_0004771 in GC patients decreased after surgery, which can track the recovery condition of patients. Besides, the downstream regulatory forecast indicates that circ_0004771 may act as miRNA sponge to regulate the progression of GC.

Conclusion: Plasma circ_0004771 can be served as a less invasive tumor biomarker with high diagnostic values.

1. Background

GC is a malignant tumor which originates from the gastric mucosal epithelial. It is one of the malignant tumors with the highest morbidity and mortality in the world[1], and ranks first in the incidence of various malignant tumors in East Asian countries[2, 3]. The vast majority of gastric cancer belongs to adenocarcinoma. The early symptoms are not obvious, which similar to gastritis, gastrohelcosis and other chronic disease symptoms, and easy to be ignored[4]. At present, blood routine and fecal occult blood test are commonly used in clinical detection of GC patients. However, the false negative rate of them are higher. Besides, the specificity of GC biomarkers such as serum carcinoembryonic antigen (CEA) is not strong. Biopsy is the best diagnostic method for early GC, but it is more traumatic for patients. Therefore, the diagnosis rate of early GC is low and there is no specific tumor indicator[5-7]. It is on the urgent to find specific and sensitive diagnostic markers for gastric cancer.

CircRNAs are endogenous non-coding RNAs that are widely expressed in mammalian cells[8]. Sanger[9, 10] first discovered covalently closed circRNAs in plant viruses in the 1970s. However, due to the limited techniques at that time, it was believed that circRNAs were the wrong splicing products. In recent years, with the development of bioinformatics analysis and high-throughput sequencing technology (NGS), a mass of circRNAs have been found in eukaryotes, and their expression has tissue specificity[8]. CircRNAs have unique covalently closed cyclic structure and are hard to be digested by exonuclease. Therefore, the expression of circRNAs in cells is stable and abundant. Studies have shown that circRNAs are specifically expressed in peripheral blood of patients with gastric cancer[11]. The stable loop structure of circRNAs extend their half-life, particularly in cell-free samples (such as blood, urine and saliva), whose expression is related to tumor progression, and can be used as a molecular marker specific for the diagnosis of GC[3, 11]. Meanwhile, circRNAs have been reported to have a number of important roles including acting as protein sponges[12, 13], serving as miRNA sponges[14], and being translated into proteins or peptides[15, 16]. So far, there is increasing evidence that circRNAs are closely related to tumor microenvironment and metastasis of various cancers[17-19]. For example, circRGNEF promotes the progression of bladder cancer through the regulation of miR-548/KIF2C axis[20]. In non-small cell lung cancer, CircRNABIRC6 promotes tumor progression of by acting

as a sponge of microRNA-145[21]. CircSAMSAP1 promotes the tumor growth of colorectal cancer through miR-328-5p/E2F1 axis[22].

Our study showed that the expression level of plasma circ_0004771 in GC patients was significantly up-regulated, which has a good diagnostic efficacy in identifying GC patients, precancerous patients and gastritis patients. Therefore, circ_0004771 provides a potential possibility for early and rapid diagnosis of GC.

2. Materials And Methods

2.1 CircRNA sequencing

Hipure Total RNA MiniKit (Magen, guangzhou, China) was used to extract Total RNA from tissue samples. Concentrations and integrity total RNA were determined using a Qubit 3.0 Fluorometer (Invitrogen, Carlsbad, California) and Agilent 2100 Bioanalyzer (Applied Biosystems, Carlsbad, CA). After ribosomal RNA (Geneseed, Guangzhou, China) was removed from the extracted total RNA, the linear RNA was removed by Rnase R digestion. KAPA RNA HyperPrep Kit with RiboErase (HMR) for Illumina (KAPA Biosystems, Inc., Woburn, MA) was used to prepare the sequencing library. Sequencing analysis of circRNA was carried out with the PE150 sequencing model Illumina Hiseq Xten.

2.2 Collection of clinical plasma and tissue specimens

All tissues and clinical specimens were collected from the clinical laboratory of affiliated hospital of Nantong University. The specimens were collected between January 2014 and December 2019. 20 pairs of gastric cancer tissue samples and their corresponding paracancerous tissues were taken from the Department of General surgery, affiliated hospital of Nantong University. Tissue samples were removed and immediately stored at -80℃ with nucleic acid fixator BIOTEKE (Nantong, China). The plasma samples included 120 cases of GC patients, 40 cases of precancerous lesions, 40 cases of gastritis, 40 cases of postoperative gastritis, and 120 cases of age-matched healthy control group. The precancerous lesions were mainly collected from patients with gastric stromal tumor. Postoperative specimens were collected from patients 1 week after gastrectomy. In this study, all patients were diagnosed as GC by professional pathologists and clinicians and did not receive chemotherapy or radiotherapy before surgery. All the above samples were collected in accordance with the Code Ethics of the World Medical Association, and informed consent was obtained for experimentation with human subjects. The study was approved by the ethics committee of the local hospital (ethical review report number: 2018-L055).

2.3 Cell culture

Human GC cell lines (HGC-27, BGC-823, MKN-1 and MKN-45) were purchased from the Stem Cell Bank of the Chinese Academy of Sciences (Shanghai, China). GES-1, human gastric epithelial cells, was used as the normal control. All cell lines were cultured in RPMI1640 medium (Corning, Manassas, VA), in which 10% fetal bovine serum (FBS, Gibco, Grand Island, NY) and 1% penicillin and streptomycin were added. All cell lines were cultured in a humidified incubator at 37℃ with 5% CO2.

2.4 RNA extraction from plasma, tissues and cells

Total RNA was extracted from 300μL plasma using the plasma extraction kit (TRIzol LS, Invitrogen, Germany) in accordance with the manufacturer's protocol. 600 ~800mg of clinical tissue samples were taken, and 1ml of TRIzol (Invitrogen, Germany) was added to cleavage and extract according to the instructions. Passable cells in good growth condition were digested with trypsin. After centrifugation and supernatant, 1ml TRIzol (Invitrogen, Germany) was added and lysed for extraction according to the instructions. RNA integrity and genomic DNA contamination were detected by standard denatured agarose gel electrophoresis. Complementary DNA was synthesized using the Revert Aid First Strand cDNA Synthesis Kit (Thermo Scientific, MA, USA).

2.5 Reverse transcription and real-time fluorescent quantitative PCR

After total RNA extraction, Thermo Fisher Science reverse transcription kit was used to prepare a 20μL reverse transcription system, which was incubated at 25℃ for 5 minutes, 42℃ for 60 minutes and 70℃ for 5 minutes to obtain cDNA. Roche Light Cycler 480 (Roche, Switzerland) was used for RTFQPCR reaction. The total value of each reaction system was 20μL, including 10μL of SYBR Green I Mix (Roche), 0.5μL of primer, 2μL of cDNA and 7μL of enzyme-free water. Primers used in this study were synthesized by Sangon Biotech Corporation (Shanghai, China). Objective gene sequence circ_0004771: former primer, 5'-AGTTGCTCCAA TGACAGAGTTACC-3' and reverse primer, 5'-CCTCCTTCAGTC AAGTGTGCATC-3'; Internal reference 18s: former primer: 5'-CGGCTACCACA TCCAAGGAA-3' and reverse primer, 5'- GCTGGAA TTACCGCGGCT-3'. The relative expression of circ_0004771 was calculated by $2^{-\Delta\Delta CT}$ method, ΔΔCt=mean of experimental group ($Ct_{Circ\_0004771}$ - $Ct_{18S\ rRNA}$) and control group ($Ct_{Circ\_0004771}$-$Ct_{18S\ rRNA}$).

2.6 Exonuclease digestion experiment

10μg total RNA were extracted from MKN-1 cells and 3-4U/μg Rnase R enzyme was added. To configure the Reaction system, add 5μg 10×Reaction Buffer and the enzyme-free water until the total system is 50μL. The reaction mixture was then incubated at 37℃ for 30 minutes. The mixture was incubated at 70℃ for 10 minutes to deactivate the enzyme and reverse transcription.

2.7 Actinomycin D assay

The concentration of 1mg/ml actinomycin D was diluted to a concentration of 2.5 μg/ml using Complete Medium. The culture medium in the six-well plate was replaced by the finished culture medium containing actinomycin D, and TRIzol was added to the plate without any treatment for 0h. RNA was extracted by adding TRIzol successively at 1h,2h,4h,6h and 8h.

2.8 Nuclear and cytoplasmic RNA separation assay

Appropriate number of cells were washed with PBS twice and the supernatant was absorbed. Add 400μL Cell Fractionation Buffer, mix gently and stewing for 5-10 minutes. 500g centrifuge for 3 minutes and drain the supernatant to the collecting tube. Add 400μL Cell Disruption Buffer. Add 400μL binding solution to the cracking solution and mix it upside down. And then we add 400μL anhydrous ethanol. The mixed solution was transferred to adsorption column for filtration and centrifuged at 1000rpm for 30s. Join 700μL Wash Solution Ⅰ, 1000rpm centrifuged 30s. Add 500μL Wash Solution Ⅱ/Ⅲ, 1000rpm centrifuge 30s for 2 times. Place the adsorption column in a new collection tube, add 40μL Elution Solution (preheated at 95℃), and centrifuge at 1000rpm for 30s. Finally, added 10μL Elution Solution (preheated at 95℃) and centrifuged at 1000rpm for 30s.

2.9 Statistical analysis

SPSS 20.0 software (IBM SPSS Statistics, Chicago, USA) was used for statistical analysis. The relative expression of serum circ_0004771 in patients with different gastric diseases was expressed as mean ± standard deviation. For comparison of two independent samples, two-sided Test was adopted, while for comparison of multiple independent samples, one-way analysis of variance was adopted. The relationship between circ_0004771 and pathological parameters was analyzed by chi-square test. ROC curve and area under the curve (AUC) were used to evaluate the diagnostic efficacy of serum circ_0004771 in the diagnosis of gastric cancer. $P<0.05$ indicated that the difference was statistically significant. Graphpad Prism7 (Graphpad Software, La Jolla, CA) for drawing.

3. Results

3.1 Expression profile of circRNAs in GC tissues and paracancer tissues

To study the expression profile of circRNAs in GC tissues, we conducted circRNA sequencing in three pairs of GC tissues and paracancerous normal tissues and identified 27,870 circRNAs (GSE131414) (**Figure 1A**). According to the principle of expression difference multiple >2.0 and $P<0.05$, 2007 circRNAs were further screened (**Figure 1B**). Excluding 936 undefined circRNAs, 663 circRNAs were up-regulated and 408 circRNAs were down-regulated in GC patients. In combination with CircRNA

Db, CircBase and CircBank databases, we selected circ_0004771 with length of 203bp for subsequent research. First, we detected the expression level of circ_0004771 in 20 pairs of tissue samples, and the results showed that the expression level of circ_0004771 in GC tissues is higher than that of the adjacent normal tissues (**Figure 1C**), which was consistent with the circRNA sequencing results. Next, we detected the expression level of circ_0004771 in GC cell lines (HGC-27, MKN-45, BGC-823 and MKN-1) (**Figure 1D**). The results showed that the expression level of circ_0004771 in MKN-1 has the highest fold change. In recent years, researchers have found that more and more circRNAs can be detected in human body fluids. For example, plasma circARS can be used as a biomarker to monitor tumor development and progression in prostate cancer[23]. Serum circSETDB1 can be used as a non-invasive biomarker for detecting the tumor progression of high grade serous ovarian cancer (SOC) patients and predict the response and recurrence to chemotherapy[24]. Serum circFoxO3a can act as a potential noninvasive prognostic biomarker and therapeutic target[25]. Therefore, we want to explore the possibility of plasma circ_0004771 as a biomarker. First, we detected the expression level of circ_0004771 in the plasma of 20 GC patients, revealing that the relative expression of circ_0004771 in the plasma of GC patients is higher than that of healthy group (**Figure 1E**). Next, we observed a well correlation of the circ_0004771 expression between tissues and plasma of GC patients ($P<0.01$, $R^2=0.6706$) (**Figure 1F**). In order to further explore that plasma circ_0004771 originate from GC cells, we found that with the longer culture time of GC cells in the culture flasks, the relative expression of circ_0004771 in the supernatant of SGC-7901 and MKN-1 increased gradually, especially in SGC-7901. While there was no significant change in the relative expression of circ_0004771 in the supernatant of GES-1. It suggested that circ_0004771 may be released into the blood by GC cells. (**Figure 1G**).

3.2 Advantages of plasma circ_0004771 as a diagnostic biomarker

Circ_0004771 is originated from the NRIP1 gene, which locates at chromosome21. It consists of the backsplicing of exon2 and exon3 (**Figure 2A**). Moreover, Sanger sequencing confirmed that the cyclization site of the amplification products is consistent with that provided in CircBase database (**Figure 2B**). The above experiments verifed that circ_0004771 has a cyclic structure. Due to its circular structure, circ_0004771 is not easily degraded by Rnase R, while the liner NRIP1 expression decreased. (**Figure 2C**). Meanwhile, the half-life of circ_0004771 after being treated with actinomycin D is longer than that of its parent gene NRIP1 (**Figure 2D**).

3.3 Plasma circ_0004771 as a biomarker for the detection of large sample size

Because the detection of circ_0004771 in plasma have no standard internal reference, we compared a series of the most commonly used internal reference such as 18S rRNA, GAPDH, β-actin, β2M, Tub and RP□ in 20 GC patients and 20 healthy examiners. Since 18S rRNA has preferable stability in both patients and healthy donors (**Supplementary Table 1**), we finally chose 18S rRNA as the endogenous reference for detecting the relative expression of circ_0004771. In order to verify that circ_0004771 is suitable for clinical laboratory analysis, we used qRT-PCR method to detect the relative expression of circ_0004771. First, we constructed a standard recombinant plasmid for circ_0004771. The regression equation of the standard curve of circ_0004771 is $y=-3.4424x + 34.732$, and R^2 is 0.9983, indicating that qRT-PCR is an effective method to detect the plasma circ_0004771 at different concentrations (**Figure 3A**). Next, we selected mixed plasma for precision determination of plasma circ_0004771. The results showed that the coefficient of variation (CV) of circ_0004771 in inter-assay is 3.59% and CV of circ_0004771 in intra-assay is 2.16% (**Table 1**). We placed the mixed plasma samples at room temperature for 0, 6, 12, 18 and 24 hours and repeated freeze-thaw for 0,1,3,5 and 10 times, and then detected the relative expression level of circ_0004771. The results revealed that there is no significant difference in the expression level of circ_0004771 in plasma ($P>0.05$), indicating that the detection of circ_0004771 had good repeatability and stability (**Figure 3B, 3C**). Finally, we correctly designed the divergent primer for circ_0004771, and the length of the amplification product of qRT-PCR is expected to be 125bp. AGE (**Figure 3D**) and melting curves (**Figure 3E**) further verified the accuracy and specificity of the amplified products. All the above results demonstrated that the detection of plasma circ_0004771 by qRT-PCR is suitable for clinical laboratory analysis.

Under this test model, we collected plasma samples from 120 GC patients, 40 precancerous lesions, 40 gastritis patients and 120 healthy donors. We found that plasma circ_0004771 expression level in GC patients was significantly higher than that in healthy controls (P<0.0001) as well as gastritis patients (P<0.0001). But there is no significant difference in the expression level of circ_0004771 between gastritis patients and healthy donors (P=0.1639). In addition, the expression level of circ_0004771 in precancerous patients is higher than that in GC patients (P=0.0356), suggesting the possibility of drug intervention before GC **(Figure 3F).**

3.4 Diagnostic utility of plasma circ_0004771 in GC

ROC curves and the AUC of ROC curves were performed on data from the 120 GC patients and 120 healthy controls to investigate the ability of plasma circ_0004771 as a diagnostic biomarker for GC. The results showed that the plasma circ_0004771 effectively distinguished the primary GC patients from the healthy subjects, and the AUC is 0.831 (95%CI: 0.779-0.883, P<0.0001) (**Figure 4A**). In addition, the AUC of plasma circ_0004771 in differentiating primary GC from gastritis patients is 0.845 (95%CI: 0.772-0.917, P=0.0356) (**Figure 4B**). Meanwhile, plasma circ_0004771 could also effectively distinguish primary GC patients from precancerous patients, with an AUC of 0.623 (95%CI: 0.524-0.722, P<0.0001) (**Figure 4C**).

Both **Figure 4D** and **Table 2** showed that the combined detection of plasma circ_0004771, CEA and CA199 in plasma is superior to any of the biomarkers detected separately in the diagnosis of GC patients and healthy subjects (AUC=0.864, sensitivity =0.79, specificity =0.78). Plasma circ_0004771 combined with CEA, a commonly used clinical diagnostic marker for GC, could improve diagnostic specificity in distinguishing GC patients from gastritis patients (AUC=0.846, sensitivity=0.66, specificity=0.85) (**Figure 4E, Table 3**).

Combined with the clinicopathological data of 120 patients with GC, we found that the high expression level of plasma circ_0004771 is related to the histological classification (P<0.0001), lymph node metastasis (P=0.009), T stage (P<0.0001) and TNM stage (P=0.016), and has little correlation with age, sex and tumor size (**Table 4**). All the above indicated that plasma circ_0004771 has high diagnostic efficiency.

3.5 Effect of plasma circ_0004771 on tumor dynamic monitoring in GC patients

To verify the dynamic relationship between plasma circ_0004771 expression and tumor progression, we compared the expression level of circ_0004771 in 20 pre-treatment GC patients with 20 post-treatment patients. As is shown in **Figure 5A**, plasma circ_0004771 in primary GC patients was abnormally expressed and dynamic decreased after surgical treatment. Meanwhile, the expression level of plasma circ_0004771 was still up-regulated in patients with postoperative recurrence. All the above suggested the potential of plasma circ_0004771 in dynamic monitoring of GC patients.

3.6 Forecast the downstream regulatory network of circ_0004771 in GC

CircRNAs in the nucleus mainly regulates the transcription of parent genes, while circRNAs in the cytoplasm mainly play the role as competitive endogenous RNA (ceRNA)[26]. Using nucleo-cytoplasmic separation assay, we found that circ_0004771 mainly located in the cytoplasm (**Figure 5B**), suggesting that circ_0004771 may regulate the progression of GC after transcription. Then, we predicted the potential circRNA-miRNA-mRNA axis through circRNA sequencing and bioinformatics analysis. As is shown in **Figure 5C**, ten miRNAs (miR-4298, miR-339-5p, miR-4687-3p, miR-548, miR-148p-5p, miR-3921, miR-7974, miR-1267, miR-1200, miR-4277) and their corresponding mRNAs were presented, which may provide a new direction of circ_0004771 in the regulation of GC progression. However, more experiments are needed to confirm the in-depth regulation mechanism of circ_0004771 in GC.

4. Discussion

In recent years, a series of studies have shown that circRNAs can be used as biomarkers for the diagnosis of tumors[27-29]. In this study, we selected circ_0004771 for subsequent study by combining the circRNA sequencing of three pairs of GC tissues and circRNA-related databases. Due to the lack of efficient and non-invasive biomarkers and many circRNAs can be detected

in human body fluids, we found the expression level of circ_0004771 in plasma was higher than that in healthy controls. Because there was a well correlation of circ_0004771 expression between GC tissues and plasma, we supposed that plasma circ_0004771 were released by GC cells and could be used as a diagnostic biomarker in GC. We speculated that circ_0004771 may be released from GC tissues into plasma in the following ways: (1) It can be passively released when cell death is induced by inflammation, hypoxia or anticancer treatment; (2) Circ_0004771 may also be released into blood in the form of exosomes; (3) In addition, hormones and chemotherapy also destroy the endothelial matrix structure, which may also contribute to the release of circ_0004771 into the circulatory system.

The expression level of plasma circ_0004771 was significantly higher than healthy donors as well as gastritis. ROC analysis implied that circ_0004771 could well distinguish primary GC patients from healthy group as well as GC patients from gastritis patients. Plasma circ_0004771 combined with CEA and CA199 obtained the highest diagnostic sensitivity. Plasma circ_0004771 combined with CEA can effectively distinguish primary GC patients from gastritis patients with the highest specificity. The expression level of plasma circ_0004771 decreased after surgery and increased after recurrence, suggesting that plasma circ_0004771 can be used as a dynamic indicator for monitoring the progress of GC.

As a result, plasma circ_0004771 can be used as an early diagnostic criteria of GC patients and become a potential dynamic monitoring biological indicator. The prediction of circRNA-miRNA-mRNA axis illustrated that circ_0004771 may interact with ten potential miRNAs to regulate the progression of GC. Among them, miR-1267 may play a tumor inhibitory role in the occurrence and development of breast tumors, but may play a promoting role in the invasion and metastasis[30]. Besides, miR-1200 regulates tumor progression by upregulating the expression of HOXB2 in glioma[31] and osteosarcoma[32]. From these findings, we have reason to speculate that these miRNAs may also play a role in GC. However, the ceRNA mechanism of circ_0004771 remains to be confirmed in the future. The detailed investigation may help us to understand the role of circ_0004771 in tumor progression.

5. Conclusion

Plasma-derived circ_0004771, which has stable cyclic structure and longer half-time, can serve as a diagnostic biomarker in tracking the progression of gastric cancer through our comprehensive consideration. Combined diagnosis of CEA, CA199 and circ_0004771 can achieve higher diagnostic efficiency. What's more, circ_0004771 may act as miRNA sponges in the downstream regulatory of gastric cancer.

Declarations

Acknowledgements

Not applicable.

Authors' contributions

YHX collected the related paper and drafted the manuscript. SK revised the manuscript. SQJ participated in the design of the review and helped to draft and modify the manuscript. All authors read and approved the final manuscript.

Funding

This project was supported by grants from the National Natural Science Foundation of China [grant number: 81871720], Jiangsu Program for Young Medical Talents [grant number: QNRC2016695] and Jiangsu Innovation and Entrepreneurship Training Program for Undergraduates [grant number: 201810304076Y].

Availability of data and materials

The datasets used and/or analyzed during the current study are available from the corresponding author upon reasonable request.

Ethics approval and consent to participate

We obtained human GC samples and healthy samples from the Affiliated Hospital of Nantong University. The ethics committee of the Affiliated Hospital of Nantong University approved all of our experiments. All participants obtained informed consent before clinical trial and gave consent to publish.

Consent for publication

All authors have read and approved the final manuscript.

Competing interests

The authors declare that they have no competing interests.

Reference

1. Kim EJ, Baik GH. [Review on gastric mucosal microbiota profiling differences in patients with chronic gastritis, intestinal metaplasia, and gastric cancer]. The Korean journal of gastroenterology = Taehan Sohwagi Hakhoe chi 2014; 64, 390-393.
2. Shin VY, Chu KM. MiRNA as potential biomarkers and therapeutic targets for gastric cancer. World J. Gastroenterol. 2014; 20, 10432-10439.
3. Hamashima C. Current issues and future perspectives of gastric cancer screening. World J. Gastroenterol. 2014; 20, 13767-13774.
4. Karimi P, Islami F, Anandasabapathy S, Freedman ND, Kamangar F. Gastric cancer: descriptive epidemiology, risk factors, screening, and prevention. Cancer epidemiology, biomarkers & prevention : a publication of the American Association for Cancer Research, cosponsored by the American Society of Preventive Oncology 2014; 23, 700-713.
5. Sugano K. Screening of gastric cancer in Asia. Best practice & research. Clinical gastroenterology 2015; 29, 895-905.
6. Sawaki K, Kanda M, Kodera Y. Review of recent efforts to discover biomarkers for early detection, monitoring, prognosis, and prediction of treatment responses of patients with gastric cancer. Expert Rev. Gastroenterol. Hepatol. 2018; 12, 657-670.
7. Li TT, Liu H, Yu J, Shi GY, Zhao LY, Li GX. Prognostic and predictive blood biomarkers in gastric cancer and the potential application of circulating tumor cells. World J. Gastroenterol. 2018; 24, 2236-2246.
8. Memczak S, Jens M, Elefsinioti A, Torti F, Krueger J, Rybak A, Maier L, Mackowiak SD, Gregersen LH, Munschauer M, et al. Circular RNAs are a large class of animal RNAs with regulatory potency. Nature 2013; 495, 333-338.
9. Kos A, Dijkema R, Arnberg AC, van der Meide PH, Schellekens H. The hepatitis delta (delta) virus possesses a circular RNA. Nature 1986; 323, 558-560.
10. Sanger HL, Klotz G, Riesner D, Gross HJ, Kleinschmidt AK. Viroids are single-stranded covalently closed circular RNA molecules existing as highly base-paired rod-like structures. Proc. Natl. Acad. Sci. U. S. A. 1976; 73, 3852-3856.
11. Chen W, Quan Y, Fan S, Wang H, Liang J, Huang L, Chen L, Liu Q, He P, Ye Y. Exosome-transmitted circular RNA hsa_circ_0051443 suppresses hepatocellular carcinoma progression. Cancer Lett. 2020; 475, 119-128.
12. Qu S, Zhong Y, Shang R, Zhang X, Song W, Kjems J, Li H. The emerging landscape of circular RNA in life processes. RNA Biol. 2017; 14, 992-999.
13. Qu S, Yang X, Li X, Wang J, Gao Y, Shang R, Sun W, Dou K, Li H. Circular RNA: A new star of noncoding RNAs. Cancer Lett. 2015; 365, 141-148.

14. Hansen TB, Jensen TI, Clausen BH, Bramsen JB, Finsen B, Damgaard CK, Kjems J. Natural RNA circles function as efficient microRNA sponges. Nature 2013; 495, 384-388.
15. Yang Y, Fan X, Mao M, Song X, Wu P, Zhang Y, Jin Y, Yang Y, Chen LL, Wang Y, et al. Extensive translation of circular RNAs driven by N-methyladenosine. Cell Res. 2017; 27, 626-641.
16. Legnini I, Di Timoteo G, Rossi F, Morlando M, Briganti F, Sthandier O, Fatica A, Santini T, Andronache A, Wade M, et al. Circ-ZNF609 Is a Circular RNA that Can Be Translated and Functions in Myogenesis. Mol. Cell 2017; 66, 22-37.e29.
17. Zhong Z, Huang M, Lv M, He Y, Duan C, Zhang L, Chen J. Circular RNA MYLK as a competing endogenous RNA promotes bladder cancer progression through modulating VEGFA/VEGFR2 signaling pathway. Cancer Lett. 2017; 403, 305-317.
18. Chen X, Yu J, Tian H, Shan Z, Liu W, Pan Z, Ren J. Circle RNA hsa_circRNA_100290 serves as a ceRNA for miR-378a to regulate oral squamous cell carcinoma cells growth via Glucose transporter-1 (GLUT1) and glycolysis. J. Cell. Physiol. 2019; 234, 19130-19140.
19. Karedath T, Ahmed I, Al Ameri W, Al-Dasim FM, Andrews SS, Samuel S, Al-Azwani IK, Mohamoud YA, Rafii A, Malek JA. Silencing of ANKRD12 circRNA induces molecular and functional changes associated with invasive phenotypes. BMC Cancer 2019; 19, 565.
20. Yang C, Li Q, Chen X, Zhang Z, Mou Z, Ye F, Jin S, Jun X, Tang F, Jiang H. Circular RNA circRGNEF promotes bladder cancer progression via miR-548/KIF2C axis regulation. Aging 2020; 12.
21. Yang H, Zhao M, Zhao L, Li P, Duan Y, Li G. CircRNA BIRC6 promotes non-small cell lung cancer cell progression by sponging microRNA-145. Cell. Oncol. (Dordr.) 2020.
22. Zhou C, Liu HS, Wang FW, Hu T, Liang ZX, Lan N, He XW, Zheng XB, Wu XJ, Xie D, et al. circCAMSAP1 Promotes Tumor Growth in Colorectal Cancer via the miR-328-5p/E2F1 Axis. Molecular therapy : the journal of the American Society of Gene Therapy 2020; 28, 914-928.
23. Luo J, Li Y, Zheng W, Xie N, Shi Y, Long Z, Xie L, Fazli L, Zhang D, Gleave M, Dong X. Characterization of a Prostate- and Prostate Cancer-Specific Circular RNA Encoded by the Androgen Receptor Gene. Molecular therapy. Nucleic acids 2019; 18, 916-926.
24. Wang W, Wang J, Zhang X, Liu G. Serum circSETDB1 is a promising biomarker for predicting response to platinum-taxane-combined chemotherapy and relapse in high-grade serous ovarian cancer. Onco Targets Ther. 2019; 12, 7451-7457.
25. Tang X, Liu S, Ding Y, Guo C, Guo J, Hua K, Qiu J. Serum Circular FoxO3a Serves as a Novel Prognostic Biomarker in Squamous Cervical Cancer. Cancer Manag. Res. 2020; 12, 2531-2540.
26. Rong D, Sun H, Li Z, Liu S, Dong C, Fu K, Tang W, Cao H. An emerging function of circRNA-miRNAs-mRNA axis in human diseases. Oncotarget 2017; 8, 73271-73281.
27. Yang L, Yu Y, Yu X, Zhou J, Zhang Z, Ying S, Guo J, Yan Z. Downregulated Expression of hsa_circ_0005556 in Gastric Cancer and Its Clinical Significance. Dis. Markers 2019; 2019, 2624586.
28. Tao X, Shao Y, Lu R, Ye Q, Xiao B, Ye G, Guo J. Clinical significance of hsa_circ_0000419 in gastric cancer screening and prognosis estimation. Pathol. Res. Pract. 2020; 216, 152763.
29. Li T, Shao Y, Fu L, Xie Y, Zhu L, Sun W, Yu R, Xiao B, Guo J. Plasma circular RNA profiling of patients with gastric cancer and their droplet digital RT-PCR detection. J. Mol. Med. (Berl.) 2018; 96, 85-96.
30. Torkashvand S, Damavandi Z, Mirzaei B, Tavallaei M, Vasei M, Mowla SJ. Decreased Expression of Bioinformatically Predicted piwil2-targetting microRNAs, miR-1267 and miR-2276 in Breast Cancer. Arch. Iran. Med. 2016; 19, 420-425.
31. Pan B, Zhao M, Wang N, Xu L, Wu T, Li Z. LncRNA RGMB-AS1 Promotes Glioma Growth and Invasion Through miR-1200/HOXB2 Axis. Onco Targets Ther. 2019; 12, 10107-10114.
32. Li S, Pei Y, Wang W, Liu F, Zheng K, Zhang X. Circular RNA 0001785 regulates the pathogenesis of osteosarcoma as a ceRNA by sponging miR-1200 to upregulate HOXB2. Cell cycle (Georgetown, Tex.) 2019; 18, 1281-1291.

Tables

Table 1. Intra-and inter-assay CV of circ_0004771.

	circ_0004771	18S
Intra-assay CV,%	3.59%	3.94%
Inter-assay CV,%	2.16%	2.90%

Table 2. Evaluation of the diagnostic values of combination of circ_0004771, CEA, CA199 between GC patients and healthy donors.

	SEN,%	SPE,%	ACCU,%	PPV,%	NPV,%
Circ_0004771	67.50(81/120)	79.17(95/120)	73.33(176/240)	76.42(81/106)	70.90(95/134)
CEA	50.00(60/120)	75.00(90/120)	62.50(150/240)	66.67(60/90)	60.00(90/150)
CA199	30.00(36/120)	78.33(94/120)	54.17(130/240)	58.06(36/62)	52.80(94/178)
Circ_0004771+CEA	79.17(95/120)	78.33(94/120)	78.78(189/240)	78.51(95/121)	79.00(94/119)
Circ_0004771+CA199	64.17(77/120)	91.67(110/120)	77.92(187/240)	88.52(108/122)	71.90(110/153)
Circ_0004771+CEA+CA199	79.17(95/120)	78.33(94/120)	78.75(189/240)	78.51(95/121)	79.90(94/119)

Table 3. Evaluation of the diagnostic values of combination of circ_0004771, CEA, CA199 between GC patients and gastritis patients.

	SEN,%	SPE,%	ACCU,%	PPV,%	NPV,%
Circ_0004771	85.00(102/120)	80.00(32/40)	83.75(134/160)	92.73(102/110)	64.00(32/50)
CEA	50.00(60/120)	80.00(32/40)	57.50(92/160)	88.24(60/68)	34.78(32/92)
CA199	30.00(36/120)	77.50(31/40)	41.88(67/160)	80.00(36/45)	26.96(31/115)
Circ_0004771+CEA	65.83(79/120)	85.00(34/40)	70.63(113/160)	92.94(79/85)	79.00(94/119)
Circ_0004771+CA199	76.67(92/120)	67.50(27/40)	74.38(119/160)	87.62(92/105)	49.09(27/55)
Circ_0004771+CEA+CA199	75.00(90/120)	72.50(29/40)	74.38(119/160)	89.11(90/101)	49.15(29/59)

Table 4. The association between plasma circ_0004771 expression and the clinicopathological parameters in GC patients.

Parameter	No. of patients	Circ_0004771 (high)	Circ_0004771 (low)	P-value
Age				
<60	43	24	19	0.341
≥60	77	36	41	
Sex				
male	83	46	37	0.075
female	37	14	23	
Tumor size				
<5	106	51	55	0.255
≥5	14	9	5	
Differentiation grade				
Well	24	4	20	<0.0001*
Poor-moderate	96	56	40	
T stage				
T1-T2	77	28	49	<0.0001*
T3-T4	43	32	11	
Lymph node metastasis				
Positive	48	31	17	0.009*
Negative	72	29	43	
TNM stage				
□-□	93	41	52	0.016*
□-□	27	19	8	
Nerve/vascular invasion				
Positive	40	21	19	0.699
Negative	80	39	41	
CEA				
Positive	60	35	25	0.068
Negative	60	25	35	
CA199				
Positive	36	19	17	0.69
Negative	84	41	43	
PG□				
Positive	40	21	19	0.699

Negative	80	39	41	
PG□				
Positive	52	27	25	0.713
Negative	68	33	35	

Figures

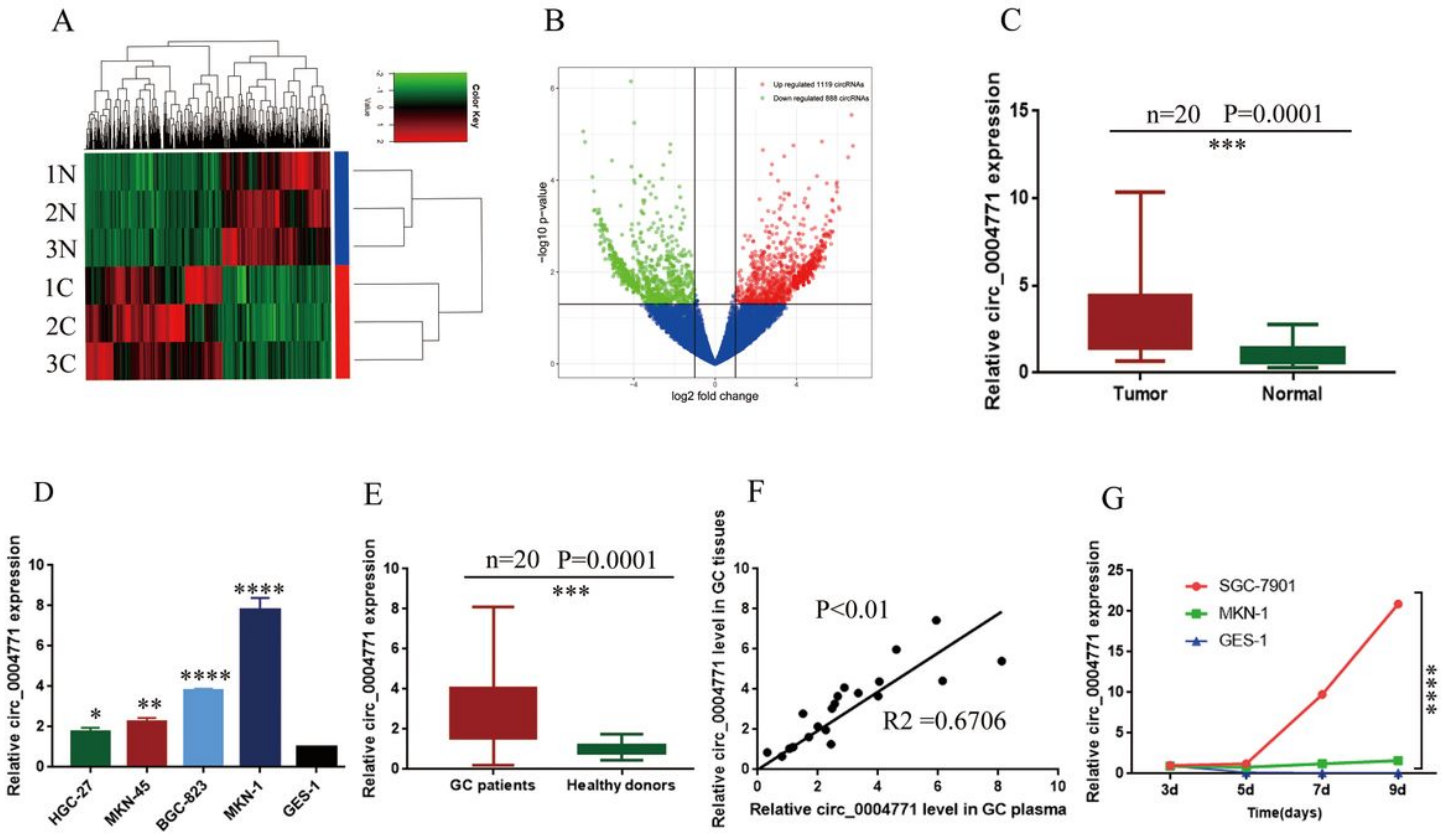

Figure 1

Expression profile of circRNAs in gastric cancer and paracancer tissues. (A) Clustered heatmap. Each row represents one specimen, and each column represents one circRNA. The color scale reflects the log2 signal strength, from green (low intensity) to black (medium intensity) to red (high intensity). (B) Volcano plots. The red dots represent statistically significant up-regulated circRNAs, the green dots represent statistically significant down-regulated circRNAs. (C) 20 pairs of tissue samples to verify the up-regulation of circ_0004771, P<0.0001. (D) Relative expression of circ_0004771 in GC cell lines. (E) Relative expression of circ_0004771 in plasma of initial 20 GC patients, P<0.0001. (F) A positive correlation of the relative expression of circ_0004771 between plasma and tissues in GC patients. (G) Expression level of circ_0004771 in culture supernatants of SGC-7901 increased with time compared to GES-1.

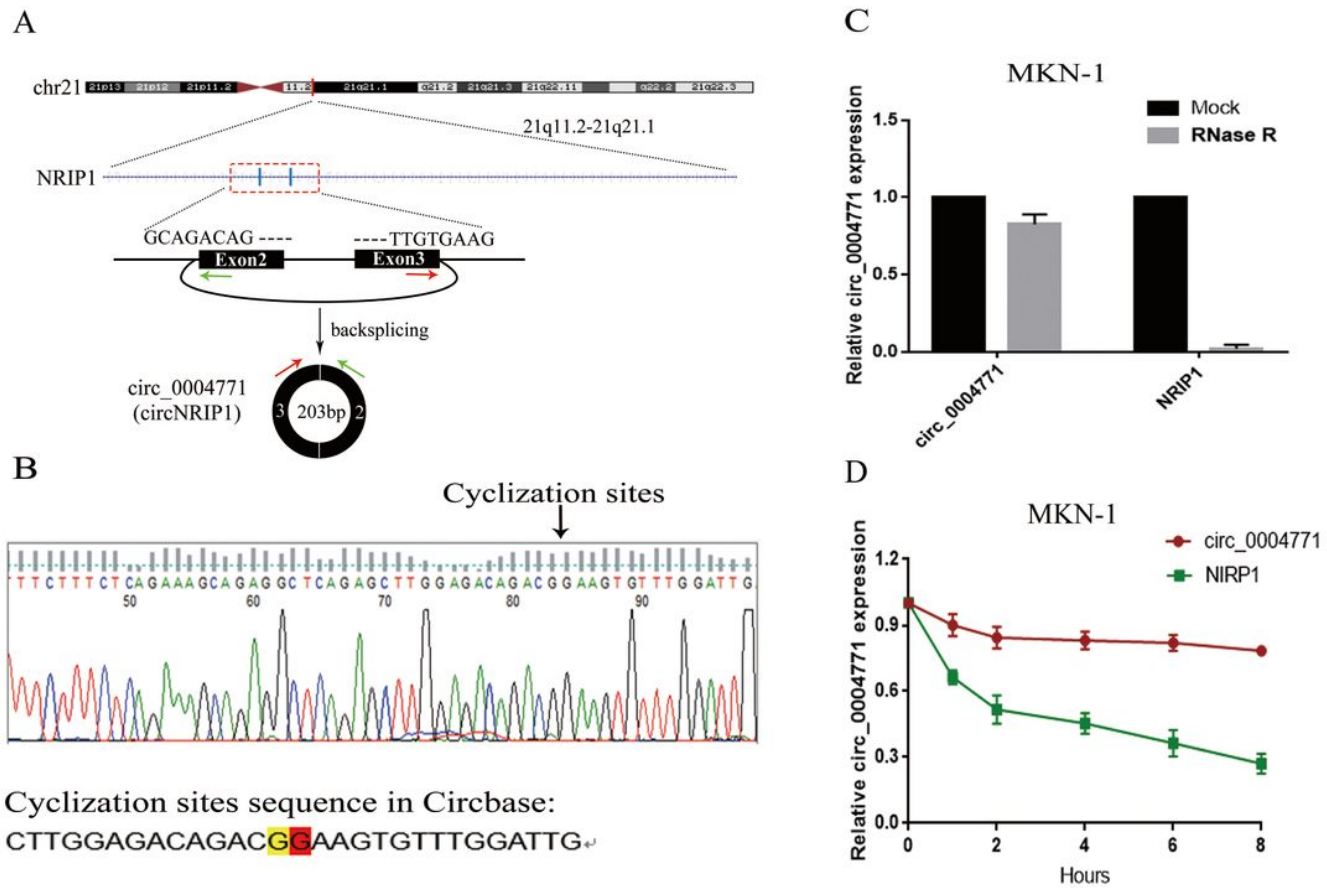

Figure 2

Identification of cyclic structure of circ_0004771. (A) Biogenesis of circ_0004771. (B) Identification of the cyclization site of circ_0004771 by Sanger sequencing. (C) Stability of circ_0004771 confirmed by Rnase R digestion assay. (D) Longer half-life of circ_0004771 verified by actinomycin D assay.

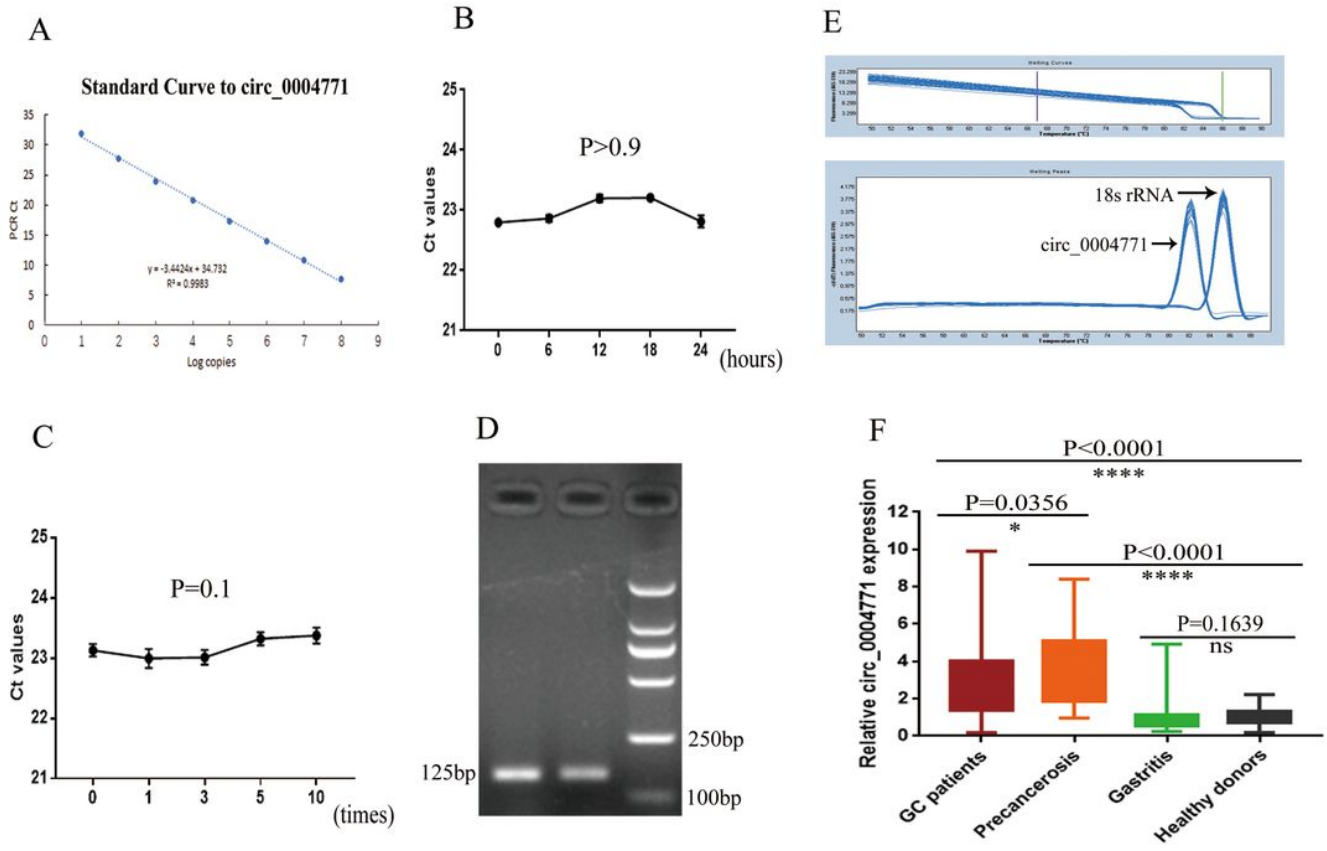

Figure 3

Construction of the research model of circ_0004771. (A) Standard curve of circ_0004771. (B) and (C) Intra-and inter-assay CV of circ_0004771 detection. Verify the accuracy and specificity of cirnc_0004771 by AGE (D) and melting curve (E). (F) Differential expression of circ_0004771 during the progression of GC.

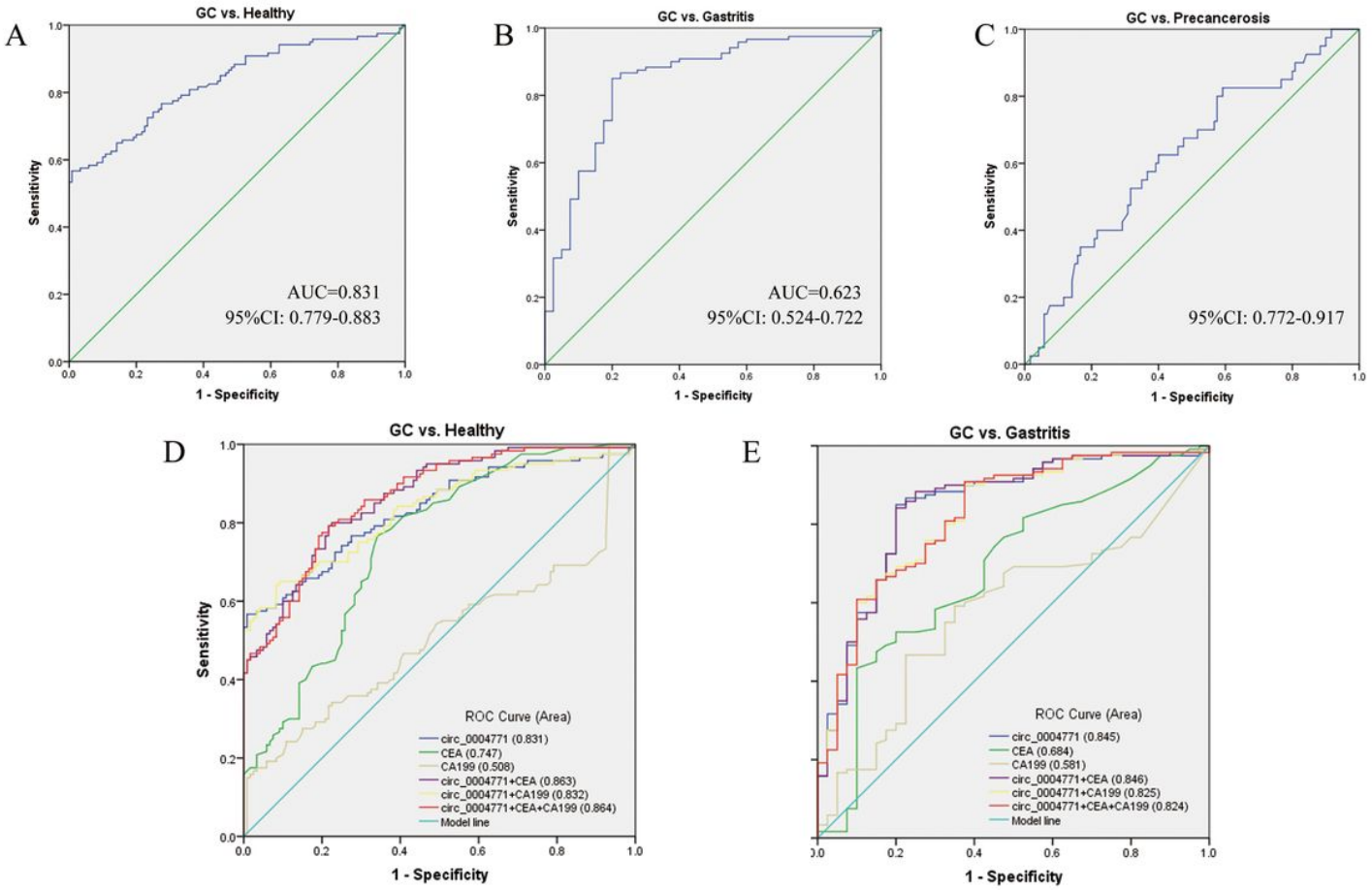

Figure 4

Potential of circ_0004771 to be a diagnostic biomarker. ROC curve analysis of plasma circ_0004771 for discriminating (A) primary GC patients and healthy donors, (B) primary GC patients and precancerosis patients, (C) primary GC patients and gastritis patients. (D) Combined diagnostic efficacy of plasma circ_0004771, CEA and CA199 exerted the best diagnostic efficiency. (E) Combined diagnostic efficacy of plasma circ_0004771 and CEA achieved a higher specificity in distinguishing GC patients and gastritis patients.

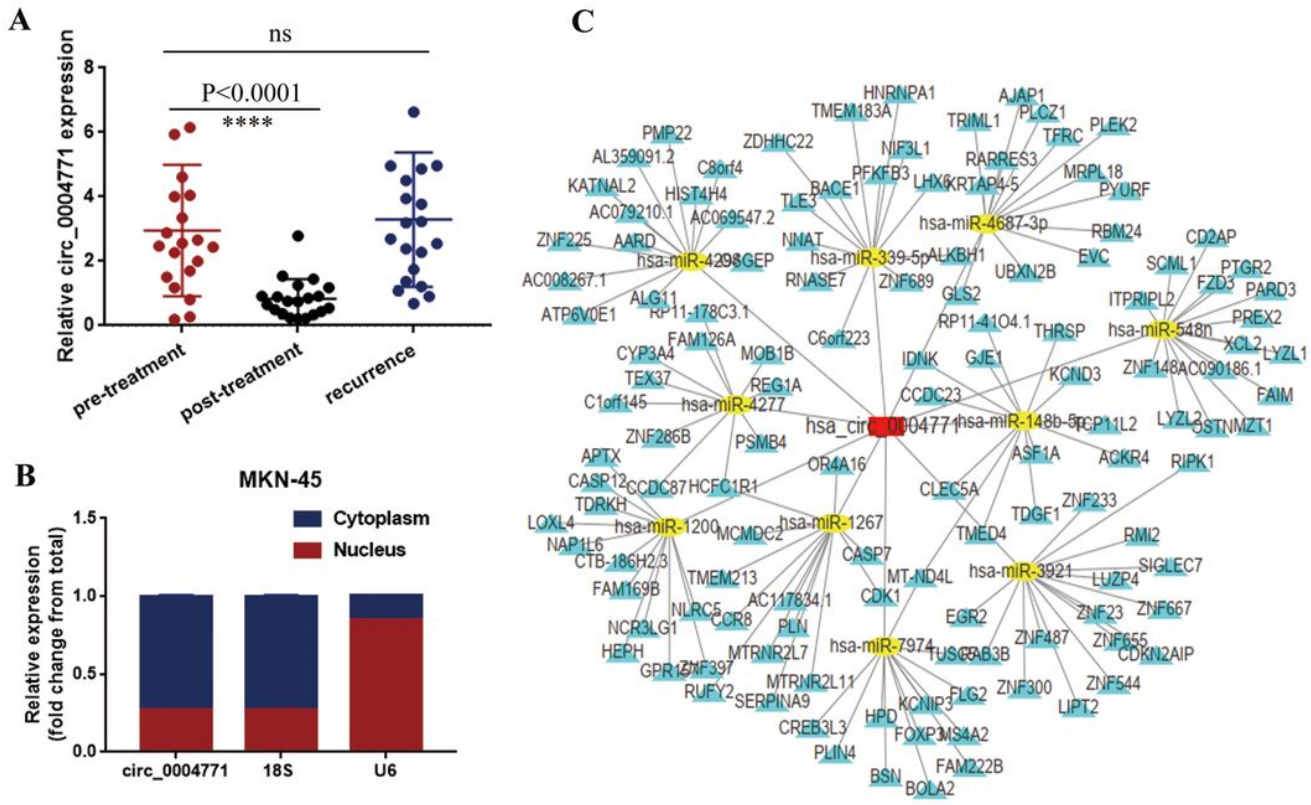

Figure 5

Dynamic monitoring and functional forecasting of circ_0004771. (A) Expression level of circ_0004771 in GC patients decreased after operation. (B) Detection of circ_0004771 location in MKN-45 cell line by nucleoplasm separation assay. (C) Prediction circRNA-miRNA-mRNA regulation network of circ_0004771. The red rectangle represents circ_0004771, and the yellow oval represents miRNAs which may bind to circ_0004771, while the yellow triangle represents the target mRNA of the corresponding miRNA.

Supplementary Files

This is a list of supplementary files associated with this preprint. Click to download.

- SupplementaryTable1.docx